Three-dimensional finite-energy Airy self-accelerating parabolic-cylinder light bullets

Wei-Ping Zhong,[1,*] Milivoj R. Belić,[2] and Tingwen Huang[2]

[1]*Department of Electronic and Information Engineering, Shunde Polytechnic, Guangdong Province, Shunde 528300, China*
[2]*Texas A&M University at Qatar, P.O. Box 23874, Doha, Qatar*

We investigate the propagation of localized three-dimensional spatiotemporal Airy self-accelerating parabolic-cylinder light bullets in a linear medium. In particular, we consider the effects resulting from utilizing initial finite-energy Airy wave packets to accelerate these localized beams in the absence of any external potential. A general localized light bullet solution with the joint Airy pulse characteristics and parabolic-cylinder spatial characteristics is obtained in the Cartesian coordinates, using parabolic-cylinder and Airy functions. Our results show that the localized wave packets can retain their intensity features and still be accelerated over several Rayleigh lengths.

I. INTRODUCTION

In 1979, Berry and Balazs realized that the force-free Schrödinger equation could give rise to solutions in the form of nonspreading Airy wave packets [1] that freely accelerate even in the absence of any external potential. In one dimension (1D), the Airy wave is the only nontrivial localized wave function that remains invariant with time [1]. The possibility of realizing such an intriguing class of beams in optics created quite a stir and it was explored in many publications [2–23]. Christodoulides and co-workers demonstrated an optical analog of Airy wave packets: specially shaped beams of light which do not diffract over long distances but could bend sideways [2,3]. Such self-accelerating Airy beams have attracted a great deal of interest, owing to their unique properties, and they provide the basis for a number of proposed applications, including optical micromanipulation [4], plasma guidance and light bullet generation [5], and routing surface plasmon polaritons [6].

Diffraction-free beams are defined as the localized optical wave packets that remain invariant during propagation. A typical example of such a diffraction-free wave is the Bessel beam, predicted theoretically and demonstrated experimentally by Durnin *et al.* in 1987 [7,8]. Such nondiffracting wave packets include various Bessel, Mathieu, and Weber beams, and their higher-order versions [9,10]. The beams that exhibit bidiffraction (part normal, part anomalous) appear in photonic lattices as nondiffracting x waves and Bessel-like beams [11–13]. These waves contain infinite power and consequently do not diffract. However, once diffractionless beams pass through finite apertures or are truncated in other ways, they eventually become diffractive. Still, the size of diffraction can be small, depending on the size of the aperture or the degree of truncation. Concerning Bessel beams, Gori *et al.* have investigated finite-beam effects in [14].

One of the problems with diffractionless wave packets is their dimensionality. Curiously, unlike nonlinear optics, in linear optics the one-dimensional (1D) wave packets are a bigger problem than the two-dimensional (2D) or three-dimensional

(3D) packets; the above-mentioned beams commonly exist in 2D and 3D. The problem arises in 1D with the diffraction of plane waves that carry infinite energy. Still, diffractionless Airy waves in 1D are possible, as first discussed by Berry and Balazs [1,15]. Such Airy waves are rather strange, in that they accelerate during propagation [3]. In fairness, it should be mentioned that actually, the whole wave packets do not accelerate, only their points of maximum field. The "center of mass" of such beams (of finite energy) moves with constant velocity. The acceleration of these beams was explained by Greenberger using the equivalence principle [16]. Recently, 3D Airy-Bessel bullets that are unaffected by both dispersion and diffraction have been suggested [3,17] and successfully demonstrated in dispersive media [5]. This versatile class of optical wave packets can exist even in 1D. They are possible irrespective of the dispersion properties of the material.

In this paper we investigate $(3 + 1)$D spatiotemporal accelerated Airy parabolic-cylinder light bullets with finite energy, in which the temporal part comes from the Airy function, and the spatial part comes from the parabolic-cylinder functions. Our results show that even in this case, the 3D wave packets can retain their intensity features and can still accelerate (in the sense mentioned) over several Rayleigh lengths. Thus, we demonstrate that a class of 3D spatiotemporal parabolic-cylinder and Airy localized wave packets exists and can self-accelerate in the absence of any external potential. Such solutions, constructed using the method of separation of variables, are written as products of complex modulation functions and Gaussian beams in Cartesian coordinates, and form localized linear light bullets that slowly expand over several diffraction lengths.

The paper is organized as follows. In Sec. II we introduce the classes of 3D spatiotemporal parabolic-cylinder and Airy localized wave packets, described by the general 3D linear Schrödinger equation in the absence of any external potential. Using the separation of variables, we construct a class of 3D spatiotemporal wave packets or linear light bullets. In Sec. III, we present some solutions as interesting examples, for some specific parameters. We find that the 3D spatiotemporal parabolic-cylinder and Airy localized wave packets can display various forms. In the final section, we summarize our results.

_____
*Corresponding author: zhongwp6@126.com
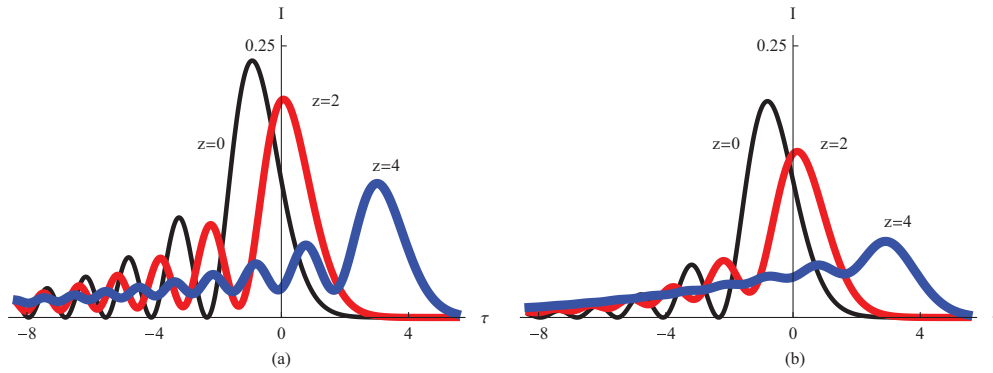
FIG. 1. (Color online) Intensity profiles of a finite-energy Airy wave packet at various propagating distances ($z = 0,2,4$) for different decay factors (a) $a = 0.1$, (b) $a = 0.2$.

II. THE MODEL AND ITS LOCALIZED WAVE-PACKET SOLUTIONS

To demonstrate a class of spatiotemporal parabolic-cylinder and Airy localized waves, we consider a 3D diffractive and dispersive optical paraxial system in a linear dielectric medium. This situation can arise in anomalous dispersive planar waveguides, where diffraction is two dimensional and paraxial propagation is perpendicular to the transverse plane. By equalizing diffraction and dispersion effects, the spatiotemporal evolution of the wave packet can be described by the $(3+1)$D linear Schrödinger equation in the absence of any external potential [3,18]:

$$i\frac{\partial V}{\partial z} + \frac{1}{2}\nabla^2 V = 0, \qquad (1)$$

where V is the complex slowly varying envelope of the optical pulse, $\nabla^2 = \frac{\partial^2}{\partial x^2} + \frac{\partial^2}{\partial y^2} + \frac{\partial^2}{\partial \tau^2}$ is the spatiotemporal Laplacian, x and y are the normalized transverse coordinates, τ stands for the local (retarded) dimensionless time in a frame of reference moving with the pulse, and z is the propagation distance in units of Rayleigh length. In Eq. (1), without any loss of generality, an anomalously dispersive system is assumed. It is interesting to note that if one interprets z as time and τ as the longitudinal coordinate, then Eq. (1) is equivalent to the Schrödinger equation for the wave function of a particle in free space, in units where m and $\hbar$ are set equal to 1. In optics, the same equation allows the propagation of wave packets of special form that are practically nondiffracting in linear dielectric media but also partially accelerating [1–3].

Equation (1) has many solutions, obtained by many solution methods. To find different solutions of Eq. (1), we resort to a partial separation of variables and assume a solution of the form

$$V(x,y,\tau,z) = T(\tau,z)u(x,y,z). \qquad (2)$$

Direct substitution of Eq. (2) into Eq. (1) gives two Schrödinger equations of lower dimensions:

$$i\frac{\partial T}{\partial z} + \frac{1}{2}\frac{\partial^2 T}{\partial \tau^2} = 0, \qquad (3a)$$

$$i\frac{\partial u}{\partial z} + \frac{1}{2}\left(\frac{\partial^2 u}{\partial x^2} + \frac{\partial^2 u}{\partial y^2}\right) = 0, \qquad (3b)$$

in the temporal and spatial domains. Further analysis may proceed along different paths. Here, we specifically investigate

the dynamics of finite-power Airy beams in the temporal τ domain, by considering a specific input into the system (at $z = 0$) of the form $T(\tau, z = 0) = \text{Ai}(\tau)\exp(a\tau)$, where $\text{Ai}(\tau)$ is the Airy function and a ($0 \leqslant a \leqslant 1$) is a decay factor. This ensures the containment of the infinite Airy tail, which enables a physical realization of the beam with finite energy [19]. The spatial dependence is confined to the beam amplitude u in Eq. (3b).

By directly solving Eq. (3a) under such an initial condition, we find that this optical pulse will evolve according to [2,19]

$$T(\tau,z) = \text{Ai}\left(\tau - \frac{z^2}{4} + iaz\right)\exp\left[a\tau - \frac{1}{2}az^2 \right.$$
$$\left. + i\left(\frac{1}{2}\tau z + \frac{1}{2}a^2 z - \frac{1}{12}z^3\right)\right]. \qquad (4)$$

Note that in the limit $a = 0$ this solution reduces to the nondispersive wave packet found in Ref. [1]. Equation (4) clearly shows that the diffraction-free Airy wave packets remain invariant during propagation, while they experience acceleration of their most intensive lobes [19]. If $a \neq 0$, Eq. (4) represents the solution in the form of a finite-energy Airy beam that slowly diffracts. Figure 1 displays intensity profiles [$I = |T(\tau,z)|^2$] of a finite-energy Airy wave packet at various propagation distances, for different decay factors a. It is seen that for small a ($\ll 1$), the beam displays similar features as the diffraction-free Airy wave packet and remains invariant over finite propagating distances. However, for nonzero a, diffraction and dissipation effects eventually take over as z increases, and the finite-energy Airy beam gradually diminishes. Crucial in this regard is the factor $\exp(-az^2)$ figuring in the intensity of the finite-energy Airy beam.

Next, we search for the spatial solution of Eq. (3b); again, this can be accomplished in many ways. We opt for a solution that is the product of a complex modulation function $u_F(z,x,y)$ and the localized Gaussian beam $u_G(z,x,y)$,

$$u(z,r) = u_F(z,x,y)u_G(z,x,y), \qquad (5)$$

where $u_G(z,r)$ is of the form [20,21]

$$u_G(z,x,y) = \frac{q_0}{q(z)}e^{-\frac{x^2+y^2}{2q(z)}}. \qquad (6)$$

Here $q(z) = z - iz_R$, $q(0) = -iz_R$, and z_R is the Rayleigh range assumed to be the unit of length. Substituting Eq. (5) into Eq. (3b) and using Eq. (6), we get an equation for u_F:

$$i\frac{\partial u_F}{\partial z} + \frac{1}{2}\left(\frac{\partial^2 u_F}{\partial x^2} + \frac{\partial^2 u_F}{\partial y^2}\right) + i\frac{1}{q}\left(x\frac{\partial u_F}{\partial x} + y\frac{\partial u_F}{\partial y}\right) = 0. \tag{7}$$

We have encountered a similar equation in our earlier work [22]. To find solutions of Eq. (7), we resort again to the separation of variables; we split Eq. (7) into two independent equations [21–24]. We obtain $(1+1)$D partial differential equations in each of the transverse dimensions, for example, in the x direction:

$$i\frac{\partial u_F}{\partial z} + \frac{1}{2}\frac{\partial^2 u_F}{\partial x^2} + \frac{i}{q}x\frac{\partial u_F}{\partial x} = 0. \tag{7a}$$

We assume $u_F(z,x) = A(z)F(\Omega)$, where $A(z)$ is the amplitude of the beam, and $\Omega(z,x) = \frac{x}{\mu(z)}$; here $\mu(z)$ is a z-dependent scaling factor, to be determined. Substituting $u_F(z,x)$ into Eq. (7a), and separating variables, one finds the following equations:

$$\frac{\partial \mu^2}{\partial z} - \frac{2\mu^2}{q} = 1, \tag{8a}$$

$$\frac{2\mu^2}{A}\frac{\partial A}{\partial z} = -\left(\lambda + \frac{1}{2}\right), \tag{8b}$$

$$\frac{\partial^2 F}{\partial \Omega^2} - i\Omega\frac{\partial F}{\partial \Omega} - i\left(\lambda + \frac{1}{2}\right)F = 0, \tag{8c}$$

where λ is the separation constant. From Eqs. (8a) and (8b), one obtains a particular solution: $\mu^2 = iz_R - z$ and $A(z) = A_0(z - iz_R)^{\frac{\lambda}{2}+\frac{1}{4}}$. Here, the choice of $A_0 = (-iz_R)^{-\frac{\lambda}{2}-\frac{1}{4}}$ normalizes the amplitude, $A(z=0) = 1$. Assuming $F(\Omega) = G(\Omega)\exp(\frac{i}{4}\Omega^2)$, Eq. (8c) is transformed into the well-known parabolic-cylinder differential equation,

$$\frac{\partial^2 G}{\partial \Omega^2} + \left(\frac{1}{4}\Omega^2 - i\lambda\right)G = 0. \tag{9}$$

There are two independent—even and odd—parabolic-cylinder functions, $G_\lambda^e(z,x)$ and $G_\lambda^o(z,x)$, that are the solutions to Eq. (9) [25]:

$$G_\lambda^e(\Omega) = e^{-i\frac{\Omega^2}{4}}{}_1F_1\left(\frac{1}{4} + \frac{i}{2}\lambda, \frac{1}{2}, \frac{i\Omega^2}{2}\right), \tag{10a}$$

$$G_\lambda^o(\Omega) = \Omega e^{-i\frac{\Omega^2}{4}}{}_1F_1\left(\frac{3}{4} + \frac{i}{2}\lambda, \frac{3}{2}, \frac{i\Omega^2}{2}\right), \tag{10b}$$

where ${}_1F_1$ is the confluent hypergeometric function. If we choose $\lambda = i(n + 1/2)$, these solutions can be rewritten as

$$G_n^e(z,x) = e^{-i\frac{x^2}{4(iz_R-z)}}{}_1F_1\left[-\frac{n}{2}, \frac{1}{2}, \frac{ix^2}{2(iz_R-z)}\right], \tag{11a}$$

$$G_n^o(z,x) = \frac{x}{\sqrt{(iz_R - z)}}e^{-i\frac{x^2}{4(iz_R-z)}}$$
$$\times {}_1F_1\left[-\frac{n-1}{2}, \frac{3}{2}, \frac{ix^2}{2(iz_R-z)}\right]. \tag{11b}$$

Note that we have changed the subscript to n in Eq. (11), which can be taken as an integer. Hence, n can be interpreted as the quantum number of the beam mode along the x-axis direction.

TABLE I. Different possible combinations of the exact analytical solution (13).

Type	Solution combination
1	$G_n^e(z,x)G_m^e(z,y)$
2	$G_n^o(z,x)G_m^o(z,y)$
3	$G_n^o(z,x)G_m^e(z,y)$
4	$G_n^e(z,x)G_m^0(z,y)$

By collecting the partial results and rearranging the terms, we obtain the solution to Eq. (7a):

$$u_F^{(e,o)}(z,x) = \left(1 + i\frac{z}{z_R}\right)^{\frac{i}{2}(n+\frac{1}{2})+\frac{1}{4}}e^{\frac{ix^2}{4(iz_R-z)}}G_n^{(e,o)}(z,x), \tag{12a}$$

where $G_n^{(e,o)}$ is determined by Eq. (11).

Using the same process, we obtain the following solution of Eq. (7) along the y-axis direction:

$$u_F^{(e,o)}(z,y) = \left(1 + i\frac{z}{z_R}\right)^{\frac{i}{2}(m+\frac{1}{2})+\frac{1}{4}}e^{\frac{iy^2}{4(iz_R-z)}}G_m^{(e,o)}(z,y), \tag{12b}$$

where $G_m^e(z,y) = e^{-i\frac{y^2}{4(iz_R-z)}}{}_1F_1[-\frac{m}{2}, \frac{1}{2}, \frac{iy^2}{2(iz_R-z)}]$ and $G_m^o(z,y) = \frac{y}{\sqrt{(iz_R-z)}}e^{-i\frac{y^2}{4(iz_R-z)}}{}_1F_1[-\frac{m-1}{2}, \frac{3}{2}, \frac{iy^2}{2(iz_R-z)}]$; here m is the quantum number of the beam mode in the y-axis direction. The complete class of 3D solutions of Eq. (1) in Cartesian

(a)

(b)
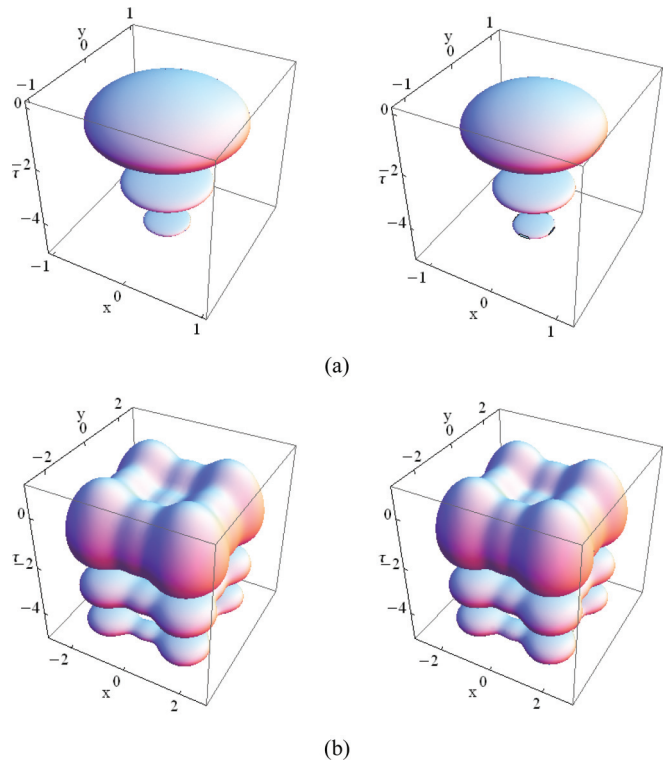
FIG. 2. (Color online) The 3D spatiotemporal localized wave-packet structures of the combination $G_n^e(z,x)G_m^e(z,y)$ and equal modal numbers. The parameters are $a = 0.1$ and (a) $n = m = 0$; (b) $n = m = 2$. The vertical (τ-axis) direction depicts the accelerating temporal direction; horizontal is the (x,y) plane. Left column is at $z = 0$, right column at $z = 5z_R$.

coordinates can be readily constructed as products of 1D solutions of the form (4) and (12),

$$V(z,x,y,\tau) = \frac{1}{1 + iz/z_R} u_F^{(e,o)}(z,x) u_F^{(e,o)}(z,y)$$

$$\times T(z,\tau) e^{-\frac{x^2+y^2}{2(z-iz_R)}}. \quad (13)$$

Thus, in Eq. (13) any combination of parities is possible. Equation (13) is the exact solution of Eq. (1). It is hence demonstrated that the shape of the spatiotemporal even and odd parabolic-cylinder Airy localized wave packets can be described by the two mode numbers (n,m).

III. ANALYSIS AND DISCUSSION

In this section, we discuss solutions given in Eq. (13) for different possible combinations of mode numbers. It should be stressed that, according to the choice of the parity, there exist four types of spatiotemporal wave packets in the form of Eq. (13) (see Table I). Thus, different classes of even and odd parabolic-cylinder Airy wave packets can be constructed by making different choices of (n,m). In the following, different combinations of the even and odd parabolic-cylinder functions are investigated.

First, we pick the even-even combination of the parabolic-cylinder functions G^e, i.e., $G_n^e(z,x)G_m^e(z,y)$. Obviously, the simplest possibility in the family of solutions given by Eq. (13) is obtained when $n = m$. Figure 2 shows the intensity of localized wave packets in the spatiotemporal three dimensions (x,y,τ) for several values of n and m, in propagation from

$z = 0$ (left column) to $z = 5z_R$ (right column), respectively. The lowest energy should occur when $n = m = 0$; the beam then forms a train of 3D ellipsoidal pulses that represent the combination of the fundamental Gaussian state with the finite-energy Airy pulse. An isosurface intensity contour plot of this wave packet is depicted in Fig. 2(a), at two z points. It is seen that the array of pulses broadens and accelerates, but stays structurally stable. In Fig. 2(b) we display the case when $n = m = 2$; there exist now similar layered structures in which four adjacent ellipsoids are connected to each other. The intensity is not zero along the τ axis for this combination. Obviously, as seen in Fig. 2, the localized wave packet accelerates along the vertical (τ-axis) direction and remains essentially invariant in the finite propagation distance. However, as mentioned above, these bullets must diffract and dissipate with the propagation distance, owing to the factor $\exp(-az^2)$ in the intensity of the finite-energy Airy beam, which figures in the overall solution. These effects are visible in the slightly diminished size of the bullets in the right column.

For the combination solution containing odd parabolic-cylinder functions G^o, $G_n^o(z,x)G_m^o(z,y)$, one obtains another class of the parabolic-cylinder and finite-energy Airy wave-packet solutions. Figure 3(a) shows the intensity distributions of such localized wave packets for the mode parameters $n = m = 1$ and Fig. 3(b) for $n = m = 4$.

Next, we investigate the intensity distributions of spatiotemporal solutions with the mixed combinations of parabolic-cylinder functions G^o and G^e. As a typical example, we choose $G_n^o(z,x)G_m^e(z,y)$. When $n = m$, the wave packets form a square matrix of ellipsoids in the horizontal plane; the structures are plotted in Fig. 4. When we choose $n = m = 1$,

(a)

(b)
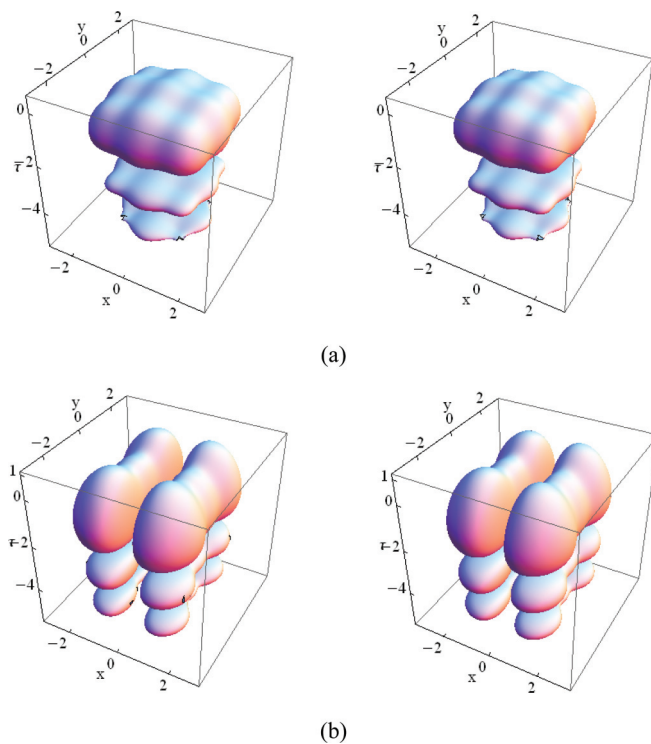
FIG. 3. (Color online) Three-dimensional spatiotemporal wave-packet solutions (13) for the combination $G_n^o(z,x)G_m^o(z,y)$. Setup and the parameters are the same as Fig. 2, except for (a) $n = m = 1$; (b) $n = m = 4$.

(a)

(b)
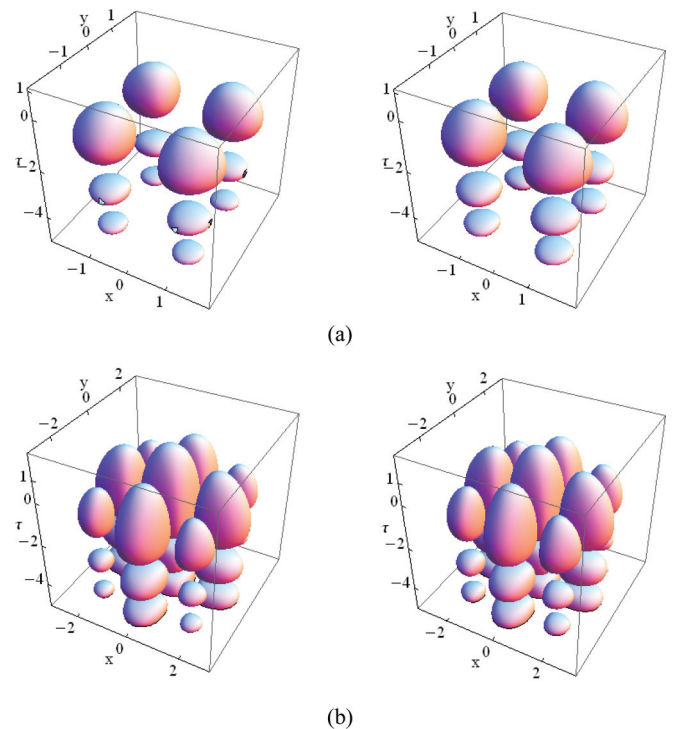
FIG. 4. (Color online) Examples of solutons (13) with the mixed combination $G_n^o(z,x)G_m^e(z,y)$. The setup and parameters are as in Fig. 2, except for (a) $n = m = 1$; (b) $n = m = 2$.

(a)

(b)
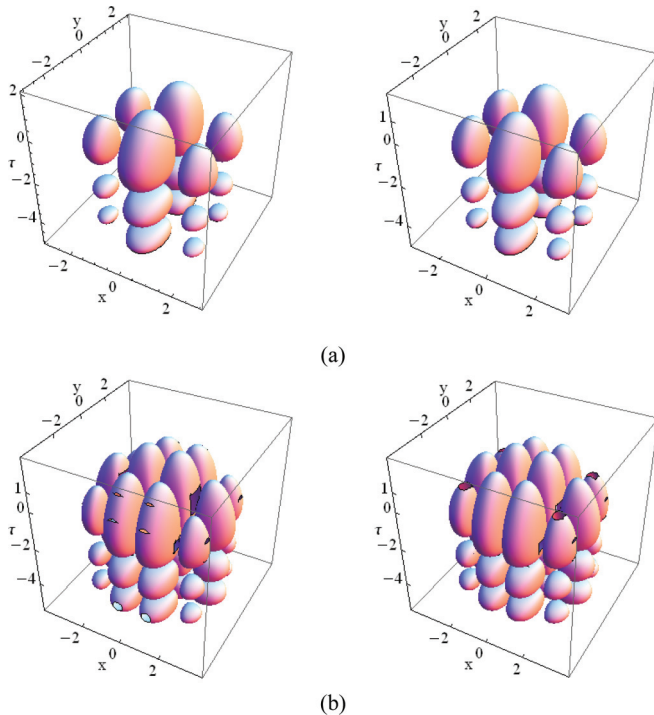
FIG. 5. (Color online) Examples of the mixed solutions (13) with unequal modal numbers. The setup and parameters are as in Fig. 4, except for (a) $n = 2, m = 1$; (b) $n = 3, m = 2$.

the 3D wave packet is composed of four ellipsoids at the same time, which form a train of pulses; the structure is presented in Fig. 4(a). In general, the 3D wave packets consist of $(n + 1)(m + 1)$ ellipsoids in the horizontal plane. If we choose $n = m = 2$, the wave packet is formed by nine ellipsoids of different sizes and shapes; see Fig. 4(b). Optical intensity is zero at the center (that is, along the τ axis) when n (or m) is odd. On the other hand, optical intensity is the maximum at the center when n is even.

Finally, we investigate the case with unequal n and m ($n \neq m$), in the mixed combination of parabolic-cylinder functions, $G_n^e(z,x) G_m^o(z,y)$. In Fig. 5, we depict some properties of the arbitrary n and m solution (13). For $n = 2$ and $m = 1$, Fig. 5(a) displays six ellipsoids in the horizontal plane. When n and m increase to $n = 3$ and $m = 2$, six ellipsoids become twelve ellipsoids that are separated from each other; see Fig. 5(b). There still exist $(n + 1)(m + 1)$ horizontal ellipsoids. The farther the position of the ellipsoid from the center of the transverse axes, the smaller the optical intensity. It is noted that the vertical (τ-axis) direction still stands as the accelerating direction.

IV. CONCLUSIONS

We have demonstrated the existence of 3D spatiotemporal finite-energy Airy parabolic-cylinder localized wave packets, which are governed by the 3D spatiotemporal linear Schrödinger equation in the absence of any external potential. These 3D localized wave packets are constructed with the aid of the well-known even and odd parabolic-cylinder and Airy functions in Cartesian coordinates, and their properties are discussed in some detail. The 3D spatiotemporal wave packets with different combinations of constituent functions may appear in different forms. We find that the localized wave packets can retain their intensity features over several Rayleigh lengths and can still accelerate along the vertical (τ-axis) direction.

[1] M. V. Berry and N. L. Balazs, Am. J. Phys. **47**, 264 (1979).

[2] G. A. Siviloglou, J. Broky, A. Dogariu, and D. N. Christodoulides, Phys. Rev. Lett. **99**, 213901 (2007).

[3] G. A. Siviloglou and D. N. Christodoulides, Opt. Lett. **32**, 979 (2007).

[4] J. Baumgartl, M. Mazilu, and K. Dholakia, Nat. Photonics **2**, 675 (2008).

[5] A. Chong, W. H. Renning, D. N. Christodoulides, and F. W. Wise, Nat. Photonics **4**, 103 (2010).

[6] A. Minovich, A. E. Klein, N. Janunts, T. Pertsch, D. N. Neshev, and Y. S. Kivshar, Phys. Rev. Lett. **107**, 116802 (2011).

[7] J. Durnin, J. Opt. Soc. Am. A **4**, 651 (1987).

[8] J. Durnin, J. J. Miceli, and J. H. Eberly, Phys. Rev. Lett. **58**, 1499 (1987).

[9] J. C. Gutiérrez-Vega, M. D. Iturbe-Castillo, and S. Chávez-Cerda, Opt. Lett. **25**, 1493 (2000).

[10] M. A. Bandres, J. C. Gutiérrez-Vega, and S. Chávez-Cerda, Opt. Lett. **29**, 44 (2004).

[11] J. Lu and J. F. Greenleaf, IEEE Trans. Ultrason. Ferroelectr. Freq. Control **39**, 19 (1992).

[12] D. N. Christodoulides, N. K. Efremidis, P. Di Trapani, and B. A. Malomed, Opt. Lett. **29**, 1446 (2004).

[13] O. Manela, M. Segev, and D. N. Christodoulides, Opt. Lett. **30**, 2611 (2005).

[14] F. Gori, G. Guattari, and C. Padovani, Opt. Commun. **64**, 491 (1987).

[15] A. Buchleitner, D. Delande, and J. Zakrzewski, Phys. Rep. **368**, 409 (2002).

[16] D. M. Greenberger, Am. J. Phys. **48**, 256 (1980).

[17] T. J. Eichelkraut, G. A. Siviloglou, I. M. Besieris, and D. N. Christodoulides, Opt. Lett. **35**, 3655 (2010).

[18] O. V. Borovkova, Y. V. Kartashov, V. E. Labanov, V. A. Vysloukh, and L. Torner, Opt. Lett. **36**, 2176 (2011).

[19] G. A. Siviloglou, J. Broky, A. Dogariu, and D. N. Christodoulides, Opt. Lett. **33**, 207 (2008).

[20] M. A. Bandres and J. C. Gutiérrez-Vega, Opt. Lett. **30**, 2155 (2005).

[21] J. C. Gutiérrez-Vega, Opt. Express **15**, 6300 (2007).

[22] W. P. Zhong, M. R. Belić, B. A. Malomed, T. W. Huang, and G. Chen, J. Phys. B **46**, 075401 (2013).

[23] M. A. Bandres and J. C. Gutiérrez-Vega, Opt. Lett. **32**, 3459 (2007).

[24] D. Deng and Q. Guo, Phys. Rev. E **84**, 046604 (2011).

[25] D. Zwillinger, *Handbook of Differential Equations*, 3rd ed. (Academic Press, Boston, 1997).